Preprint Title	Small protein sequences can induce cellular uptake of complex nanohybrids
Authors	Jan-Philip Merkl, Malak Safi, Christian Schmidtke, Fadi Aldeek, Johannes Ostermann, Tatiana Domitrovic, Sebastian Gärtner, John E. Johnson, Horst Weller and Hedi Mattoussi
Publication Date	27 Sep 2019
Article Type	Letter
Supporting Information File 1	Gamma-Peptide-Hybrids - BJNANO - SI.DOC; 3.5 MB
ORCID® iDs	Jan-Philip Merkl - https://orcid.org/0000-0003-4856-967X

Small protein sequences can induce cellular uptake of complex nanohybrids

Jan-Philip Merkl,*,[1-3] Malak Safi,[1], # Christian Schmidtke,[3] Fadi Aldeek,[1], ¶ Johannes Ostermann,[2,4] Tatiana Domitrovic, [5],& Sebastian Gärtner, [2,6] John E. Johnson, [6] Horst Weller,[2-4] and Hedi Mattoussi.[1]

Address: [1]Department of Chemistry and Biochemistry, Florida State University, 95 Chieftan Way, Tallahassee, Florida 32306 (United States)

[2]Institute of Physical Chemistry; University of Hamburg, Grindelallee 117, 20146 Hamburg

[3]The Hamburg Center for Ultrafast Imaging, University of Hamburg, Luruper Chaussee 149, 22761 Hamburg (Germany)

[4]Center for Applied Nanotechnology (CAN) GmbH, Grindelallee 117, 20146 Hamburg (Germany)

[5]The Scripps Research Institute, Department of Integrative Structural and Computational Biology, MB31, La Jolla, California 92037, (United States)

[6] Universitätsklinikum Hamburg Eppendorf, 20246, Martinistraße 52, 20251 Hamburg (Germany)

¶current address: Altria Center for research and technology, 601 E Jackson Street, Richmond, VA, 23219 (United States).

#current address: Laboratoire Physique des Solides, UMR 8502, Université de Paris Sud bât 510, 91405 Orsay Cedex (France).

&current address: Instituto de Microbiologia Paulo de Goes, Universidade Federal do Rio de Janeiro, 310. Lab I014, 21941-902, Rio de Janeiro (Brazil)

Email: Jan-Philip Merkl – janphilip.merkl@gmail.com

Abstract

In this letter, we highlight that a low fraction of functional fusion proteins can significantly change the interaction of complex nanohybrids with cells and induce cellular uptake.

Keywords

Nanoparticle hybrids, polymer encapsulation, self-assembly, cellular uptake, bioconjugation

Introduction

Developing hybrid nano-structures made of more than one component nanomaterial, combined with biomolecules is a highly sought goal in biomedical science, and can find applications in multimodal imaging and therapeutics.[1,2] Although interest in developing such hybrid nanostructures by, for example, combining plasmonic and fluorescent, or magnetic and fluorescent nanoparticles have attracted much attention for the development of bioassays, their use as cellular labelling platforms has been less explored.[2,3] Three recent demonstrations describing the use of such hybrid nanostructures in cell labelling are highlighted: In one study, Jana and co-workers reported the design of fluorescent plasmonic nanohybrids by covalent attachment of luminescent quantum dots (QDs) to Au nanorods. Further functionalization with glucose using glutaraldehyde coupling chemistry yielded nanohybrids that could subsequently be used for the staining of cellular membranes.[4] Chan and co-workers described two interesting systems. In the first, a charge driven self-assembly of

AuNPs and different-color QDs into multicolor, non-blinking nanohybrids was described. These nanohybrids were then coupled to various proteins, and among them the human transferrin protein was found to induce the highest intracellular uptake of these hybrids following 24 h incubation with the cell culture.[5] In the second, functional colloidal superstructures coupled with DNA linkers showed a reduction in the response of macrophages to these hybrids as well as improvement of in vivo tumor accumulation.[6] Weil and co-workers described the promises of multimodal platforms made of diamond dots combined with gold nanoparticles, and applied them as imaging probes of cell cultures.[7] We have recently characterized a hybrid system consisting of self-assembled gold nanoparticles (AuNPs) and polymer-encapsulated QDs. These constructs were further functionalized with polyhistidine-tagged proteins, yielding functional conjugates that exhibit fluorescent and plasmonic properties and build the basis for this letter.[8]

Over the last two decades several groups have investigated mechanisms for intra-cellular-uptake and in vivo bio-distribution of various nanomaterials.[9–11] Due to the complexity of nanostructured materials combined with the intricacy of cell biology, it has been proven very difficult to develop good understanding of what controls the processes involved in the intracellular uptake and ensuing distribution of various nanomaterials.[9] Nonetheless, it has been consistently found that NPs are very often taken up by endocytosis, and once inside the cells they remain trapped within endosomal compartments.[10,12] Still a few studies have reported that a sizable fraction of the delivered nanoparticles can end up in the cytoplasm, by either circumventing endocytosis through the use of virus-derived peptide sequences, or non-disruptively penetrating the cellular membranes such was the case for small (<5 nm) monolayer-capped AuNPs;[13] escape from endosomal vesicles of once endocytosed nanoparticles have also been discussed.[12,14,15] Additionally, it is widely accepted,

accessing colloidally stable nanoparticles is crucial for controlling cellular uptake. Conversely, materials prone to aggregation show higher non-specific interactions with live cells than their sterically-stabilized counterparts. [16,17]

In this study we report on the use of a lytic gamma peptide derived from the Nudaurelia Capensis Omega virus (NωV), which was genetically fused onto maltose binding protein appended with 7-histidine tag, (His_7-MBP-γ) to promote the intracellular delivery of hybrid QD-AuNP assemblies.[18,19] This peptide is produced during viral capsid maturation and is thought to enable cellular internalization of the virus. Indeed, it has been shown that the γ –peptide has the ability to disrupt artificial liposomes.[18,19] More recently, we have used this peptide to promote the uptake of QDs by mammalian cells.[20] Here well widen this approach to more complex hybrid structures and show, that similar results are obtained.

Results and Discussion

To assemble the biologically-active plasmonic-fluorescent platforms described in reference8 no chemical coupling was used but rather a self-assembly route that relies on direct interactions involving metal-coordination between either thiol and Au or imidazole and Au surfaces; the latter was applied to couple polyhistidine-appended maltose binding protein (MBP-His) onto the AuNPs.[8,21] Zwitterion functionalized lipoic acid-capped AuNPs (LA-ZW-AuNPs) were selected for this study, due to their compact coating, enhanced colloidal stability and reduced nonspecific-adsorption interactions.[20,22–27] The hybrids design used in this study relies on the use of QDs encapsulated with a polymer made of an amine-functionalized polyisoprene-block-polyethylene oxide (PI-b-PEO-NH2, grey region in Figure 1A) in combination with LA-ZW-AuNPs and the His_7-MBP- γ, as shown in

Figure 1A.‡ In order to demonstrate the potential for biomedical applications for this nanohybrid system, colloidal stability studies of the nanohybrid in culture media were first carried out. No aggregation was observed over a period of 5 h following dispersion in cell culture media, as verified using dynamic light scattering measurements, where mono-modal autocorrelation functions along with a single dominant hydrodynamic size were collected for the nanohybrids in cell culture media (Figure 1B).[17] In a control experiment, using citrate-stabilized AuNPs in a similar assay, the hybrid self-assembly precipitated within few minutes under the same conditions. This indicates that embedding LA-ZW-AuNPs in the hybrid enhances their colloidal stability, yielding a platform suitable for investigating nanoparticle-cell interactions. (We also proved, that no aggregation occurred by secreted biomolecules[17], as further outlined in the supporting information. Thus, we exclude the effect of aggregation as an explanation for the below discussed results.)

An amylose affinity assay was performed in order to verify that coupling of His_7-MBP-γ onto QD-AuNP hybrids occurs and that the biological activity of the MBP is preserved.[8,25,28] Once uploaded onto an amylose-filled column, the His_7-MBP-γ bearing nanohybrid bound to amylose and could not be released with several washes with buffer. The absence of both fluorescence signal (from the QDs under UV light exposure) or a pinkish colour (from the AuNPs under white light) in the eluting buffer proves that the nanohybrid is stable and the bound MBP stays functional (see Figure 1 C).[8,25,28] The bimodal character of the hybrid is reflected in the pinkish colour of the AuNPs and the fluorescence of the QDs. The nanohybrid could be readily released by adding a few mL (10-20) of maltose solution. This release is promoted by the stronger affinity of the substrate of maltose to the bound His7-MBP-γ. Further details are available in the SI and in the references 8,25,28.

After confirming the structural integrity and colloidal stability of the nanohybrids, we probed their interactions with HeLa cell cultures. For this, hybrid dispersions (consisting of 100 nM QD solution, 2 equivalents of LA-ZW-AuNP per QD and 14 equivalents His_7-MBP-γ per AuNPs, as described in the Supporting Information) were incubated with the cell culture for 1 h. A pronounced intracellular uptake of the hybrids was observed, as indicated by the significant fluorescence staining of the cells. In contrast, control experiments using hybrids prepared with gamma-free proteins (i.e., His7-MBP) did not show any cellular uptake (see Figure 1D and Figures SI 3,4).

We tested the effects of decreasing the overall concentration of the nanohybrids or the number of MBP-γ per assemblies on the uptake and staining levels of the cells. We found that reducing the overall concentration of the hybrids, the molar ratio of QD-to-AuNP in the hybrids, incubation time by 50% and substituting half of the His_7-MBP-γ with His_7-MBP (gamma-free proteins) resulted in significantly lower levels of intracellular QD staining. Flow cytometry measurements showed that under these modified conditions approx.20% of the cells are labelled with the nanohybrids. In comparison, no uptake was measured in the absence of His_7-MBP-γ (Figure SI 5).

With this decreased nanohybrid load we visualized the cell cultures using confocal microscopy imaging to gain further understanding of where the conjugates reside in the cells following uptake (Figure 1E).

We can distinguish three different colours in the images: the cell nuclei shown in blue (stained with DAPI), the endosomal compartments counterstained in red (labelled with Cy5-Transferin), and QDs in yellow. The images indicate that QDs and Cy5-transferrin do not co-localize. In addition, the dark signals observed in bright field mode, coincide with the yellow fluorescence emitted when we switch to fluorescence mode. This indicates that these spots signals are assemblies of multiple hybrid

particles, so consisting of multiple AuNPs and encapsulated QDs.[3] Similar features were reported in a recent publication of the Jana group.[4] Due to the colloidal stability of these constructs proven by DLS, which is highly sensitive for bigger aggregates, we assume, that the appearance of these big structures is due to the *cellular fate* of these structures rather than appearance in solution.

The confocal microscopy data were further exploited to generate a z-stack, to visualize the fluorescence distribution of the nanocomposites side-by-side with that of the Cy5 dye and cell nuclei. This 3D-stack (Figure 2 A) shows that the internalized nanohybrids (the yellow fluorescence staining) are distinct from the distribution of endosomes counterstained in red, thus demonstrating that the nanohybrids are not trapped within endocytic vesicles. However, it also appears, that most of the nanohybrids exhibit a certain distance to the cell nucleus – likely a cause of cell-surface adsorption of the hybrids.

Furthermore, the respective signals were identified using spectral resolution of the three associated chromophores. A spectral scan of one confocal plane is shown in Figure 2B, highlighting the different localization between nanohybrids, endosomal marker, and cell nuclei. We further applied spectral unmixing to a region, where QD fluorescence is in close proximity to the endosomal marker Cy5-transferrin (Figure 2C) underlining the above discussed unlike compartmentalization between nanohybrids and endosomal marker. All these findings show that the nanocomposites, if internalized, are found in subcellular compartments, which are not stained with the Cy5-transferrin. These results are in good agreement with our previous findings reported in reference 20. This implies that the mechanism of cellular uptake promoted by the gamma peptide is other than endocytosis.20 Still, the compartmentalized fluorescence signature of the QDs is different from that expected for *pure* cytosolic delivery, where more homogeneous distribution of the fluorescence

signal is expected.[31] Whether these findings are due to the cellular response on the NP-based structure of the hybrid or if this reflects the typical cellular fate of a non-enveloped virus is a question which cannot be addressed easily. However, it worth noting that even a small amount of γ -peptide (in average seven γ-peptide sequences per hybrid-structure) is able to promote the uptake of nanohybrids, which hydrodynamic size exceeds both the QD construct of our previous study (d(QD-LA)~10-15 nm)[20] as well as the virus itself (d~40 nm).[19] Due to their bimodal character and sensitive exciton-plasmon coupling[29] similar systems may enable to study the structural response of nanomaterials and may open up new insight in virus uptake pathways.30 Due to the complex, statistical nature of the self-assembled structures, a residual doubt Thinking one step ahead, the combination of (bio)distribution in the body (e.g. by computed tomography (CT) contrast of the AnNPs) and more detailed resolution using fluorescence microscopy may be an interesting option for biomedical diagnostics.

Experimental

‡ The synthesis and the associated spectral properties are detailed in the supporting information and in reference 1. Briefly the polymer encapsulated quantum dots are left to incubate with partially capped gold nanoparticles and subsequently functionalized with His7-MBP-γ.

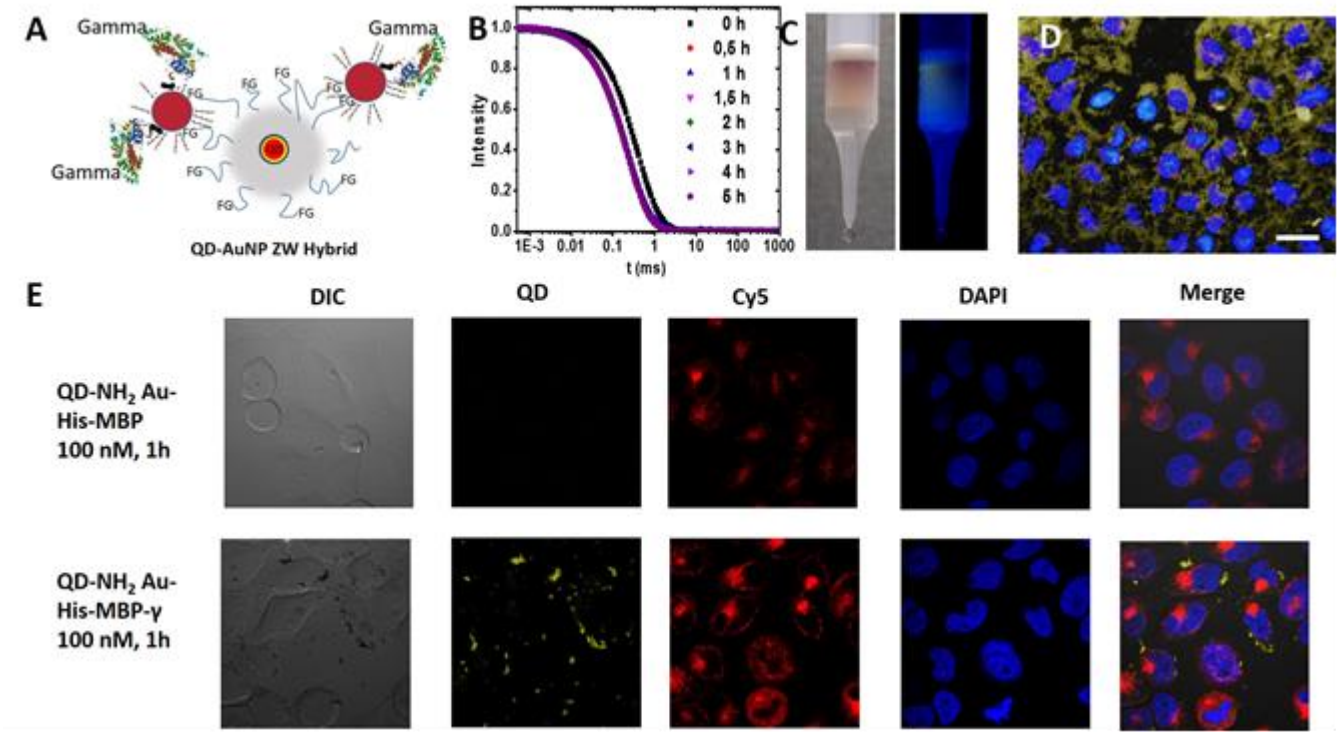

Figure 1: (A) Schematic representation of the nanohybrids (not in scale). QD is embedded in a micelle which consists of a hydrophobic moiety (grey) and an amphiphilic part (PEO). Interaction of QDs with AuNPs is driven by the functional groups (FG). Gold nanoparticles are His-conjugated to His_7-MBP-γ.[8] (B) Autocorrelation function of nanocomposite over a time period of 5 h in Dulbecco's Modified Eagle Medium (DMEM) media, indicating high colloidal stability. (C) Amylose column assay of the nanocomposite. Neither fluorescence nor pinkish color is observed in the eluting buffer, samples can be eluted by maltose solution (20 mM; not shown). (D) A representative epifluorescence image of HeLa cells after incubation of a nanocomposite, which was loaded with a high ratio (14 eq./AuNP) of His7-MBP-γ and c(QD)= 100 nM. (E) Confocal microscopy images of HeLa cells incubated with QD-NH2-Au-His7-MBP-(γ) incubated for 1 h, c(QD)= 50 nM and lower ratio of His7-MBP-γ using a 60x magnification. The scale bar represents 20 µm. (Top row) Nanocomposite with His7-MBP were used; (bottom row) nanocomposites with His7-MBP-γ were used. Shown are differential interference contrast (DIC), 4′,6-Diamidin-2-phenylindol (DAPI), Cy5, QD channels as well as an merged image. Figure 1A reprinted with permission from J. Phys. Chem. C, 2016, 120, 25732–25741. Copyright 2016 American Chemical Society.

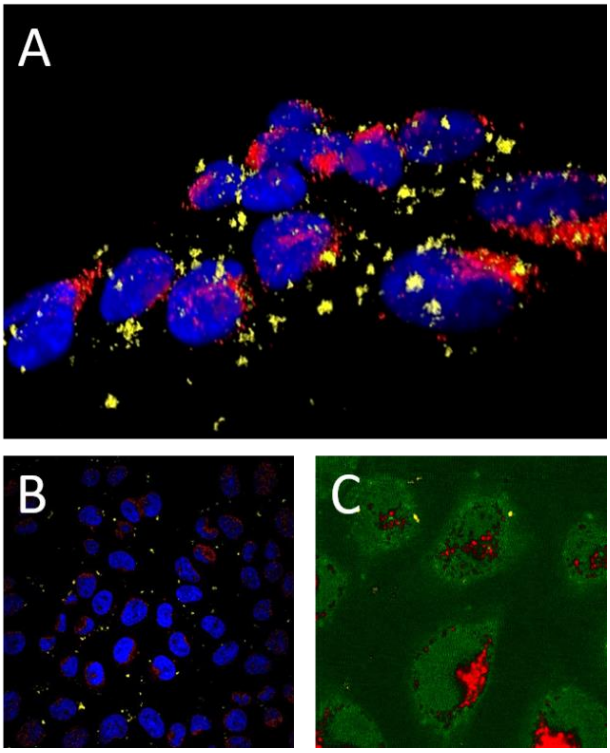

Figure 2: Confocal z- stack of HeLa cells. (A) Volume view of the confocal z-Stack, blue: DAPI, red: endosomal marker Cy5: yellow. QD signal. The displayed volume is 100 µm x 100 µm x 24 µm (B)) spectral scan of one confocal plane (same colour code) (C) spectral unmixing of QD fluorescence (575 nm) and Cy5-spectrum (red) highlighting no superposition between the QD and the Cy5 signal.

Supporting Information

† Supplementary Information (SI) available: Expression of the fusion protein His7-MBP-gamma, particle synthesize, Hybrid Assembly and Characterization, DLS characterization and colloidal stability assessment, cellular incubation, Amylose column, HeLa cellular culture, Epifluorescence z-stack, epifluorescence control experiments, flow cytometry, further Instrumentation.

Acknowledgements

This work was supported by the State Excellence Initiative “Nanotechnology in Medicine” from the Free and Hanseatic City of Hamburg and the U.S. National Science Foundation (grants NSF-CHE #1508501 and #1058957). J.-P.M., H.M. and H.W. acknowledge the support of the Chemical Industry Fund, VCI: German Chemical Industry Association and the German-American Fulbright Program. T.D. was supported by Conselho Nacional de Desenvolvimento Científico e Tecnológico (CNPq) and PEW. We also thank Goutam Palui, Xin Ji, Megan Muroski (at Florida State University), Ning Fang (Iowa State University) and John Zentmeyer (Nikon Corporation) for helpful discussions.

References

1 M. J. Sailor and J.-H. Park, Adv. Mater., 2012, 24, 3779–3802.

2 N. C. Bigall, W. J. Parak and D. Dorfs, Nano Today, 2012, 7, 282–296.

3 A. S. Stender, K. Marchuk, C. Liu, S. Sander, M. W. Meyer, E. a Smith, B. Neupane, G. Wang, J. Li, J.-X. Cheng, B. Huang and N. Fang, Chem. Rev., 2013, 113, 2469–527.

4 S. Basiruddin, A. R. Maity, A. Saha and N. R. Jana, J. Phys. Chem. C, 2011, 115, 19612–19620.

5 F. Song, P. S. Tang, H. Durst, D. T. Cramb and W. C. W. Chan, Angew. Chemie Int. Ed., 2012, 51, 8773–8777.

6 L. Chou, K. Zagorovsky and W. Chan, Nat. Nanotechnol., 2014, 9, 148–155.

7 W. Liu, B. Naydenov, S. Chakrabortty, B. Wuensch, K. Hübner, S. Ritz, H. Cölfen, H. Barth, K. Koynov, H. Qi, R. Leiter, R. Reuter, J. Wrachtrup, F. Boldt, J. Scheuer, U. Kaiser, M. Sison, T. Lasser, P. Tinnefeld, F. Jelezko, P. Walther, Y. Wu and T. Weil, Nano Lett., 2016, 16, 6236–6244.

8 J.-P. Merkl, C. Schmidtke, F. Aldeek, M. Safi, A. Feld, H. Kloust, H. Mattoussi, H. Lange and H. Weller, J. Phys. Chem. C, 2016, *120*, 25732–25741..

9 M. Nazarenus, Q. Zhang, M. G. Soliman, P. del Pino, B. Pelaz, S. Carregal-Romero, J. Rejman, B. Rothen-Rutishauser, M. J. D. Clift, R. Zellner, G. U. Nienhaus, J. B. Delehanty, I. L. Medintz and W. J. Parak, Beilstein J. Nanotechnol., 2014, 5, 1477–1490.

10 T.-G. Iversen, T. Skotland and K. Sandvig, Nano Today, 2011, 6, 176–185.

11 S. Wilhelm, A. J. Tavares, Q. Dai, S. Ohta, J. Audet, H. F. Dvorak and W. C. W. Chan, Nat. Rev. Mater., 2016, 1, 16014.

12 L. Treuel, X. Jiang and G. U. Nienhaus, J. R. Soc. Interface, 2013, 10, 1742–62.

13 A. A. Sousa, S. A. Hassan, L. L. Knittel, A. Balbo, M. A. Aronova, P. H. Brown, P. Schuck and R. D. Leapman, Nanoscale, 2016, 8, 6577–6588.

14 E. Cabane, X. Zhang, K. Langowska, C. G. Palivan and W. Meier, Biointerphases, 2012, 7, 9.

15 J. B. Delehanty, H. Mattoussi and I. L. Medintz, Anal. Bioanal. Chem., 2009, 393, 1091–105.

16 M. Safi, J. Courtois, M. Seigneuret, H. Conjeaud and J.-F. Berret, Biomaterials, 2011, 32, 9353–63.

17 A. Albanese, C. D. Walkey, J. B. Olsen, H. Guo, A. Emili and W. C. W. Chan, ACS Nano, 2014.

18 M. a Canady, M. Tihova, T. N. Hanzlik, J. E. Johnson and M. Yeager, J. Mol. Biol., 2000, 299, 573–84.

19 T. Domitrovic, T. Matsui and J. E. Johnson, J. Virol., 2012, 86, 9976–82.

20 M. Safi, T. Domitrovic, A. Kapur, N. Zhan, F. Aldeek, J. E. Johnson and H. Mattoussi, Bioconjug. Chem., 2017, 28, 64–74.

21 F. Aldeek, M. Muhammed and G. Palui, ACS Nano, 2013, 7, 2509–2521.

22 H.-S. Han, J. D. Martin, J. Lee, D. K. Harris, D. Fukumura, R. K. Jain and M. Bawendi, Angew. Chem. Int. Ed. Engl., 2013, 52, 1414–9.

23 K. Pombo García, K. Zarschler, L. Barbaro, J. a Barreto, W. O'Malley, L. Spiccia, H. Stephan and B. Graham, Small, 2014, 10, 2516–29.

24 D. F. Moyano, K. Saha, G. Prakash, B. Yan, H. Kong, M. Yazdani and V. M. Rotello, ACS Nano, 2014, 8, 6748–6755.

25 N. Zhan, G. Palui, H. Grise, H. Tang, I. Alabugin and H. Mattoussi, ACS Appl. Mater. Interfaces, 2013, 5, 2861–2869.

26 F. Aldeek, M. A. H. Muhammed, G. Palui, N. Zhan and H. Mattoussi, ACS Nano, 2013, 7, 2509–2521.

27 N. Zhan, G. Palui and H. Mattoussi, Nat. Protoc., 2015, 10, 859–874.

28 F. Aldeek, M. Safi, N. Zhan, G. Palui and H. Mattoussi, ACS Nano, 2013, 7, 10197–10210.

29 C. Strelow, T. S. Theuerholz, C. Schmidtke, M. Richter, J.-P. Merkl, H. Kloust, Z. Ye, H. Weller, T. F. Heinz, A. Knorr and H. Lange, Nano Lett., 2016, 16, 4811–4818.

30 B. Tsai, Annu. Rev. Cell Dev. Biol., 2007, 23, 23–43.

31 A. Kapur, S. Medina, W. Wang, G. Palui, X. Ji, J.P. Schneider, and H. Mattoussi, ACS Omega 2018, 3, 17164-17172.